

CONDENSATED FERMION SYSTEM IN THE MODEL OF FOUR-QUARK INTERACTION WITH LARGE CORRELATION LENGTH

S. V. Molodtsov*

Joint Institute for Nuclear Research, Dubna, Moscow region, RUSSIA

G. M. Zinovjev

Bogolyubov Institute for Theoretical Physics, National Academy of Sciences of Ukraine, Kiev, UKRAINE

(Dated: February 26, 2022)

Studying a model of four-quark interaction with large correlation length we find out both the features peculiar an unitary fermi gas and the specific anomalous properties of the fermi systems with a fermion condensate. It is argued that a possibility of phase transition originated by interface between the Fermi sphere and fermion condensate appears in such quark systems. The results obtained could be instrumental for phenomenological applications in view of our conclusion about approximately the same behavior of the dynamical characteristics of quark ensembles with different four-quark interaction forms in a practical interval of coupling constant.

PACS numbers: 11.10.-z, 11.15.Tk

A new form of matter created in ultra-relativistic heavy ion collisions at RHIC and LHC has been realized as a strongly coupled system in an anisotropic state with rather unexpected features and certainly making qualitative insights to the nature of quark-gluon plasma (QGP). The dynamical evolution of this hot and dense system being successfully analysed with the relativistic viscous hydrodynamics designates another challenge to the QGP (and QCD) theory definitely compelling to think of the QGP rather as a liquid than a gas of quarks and gluons. The present letter is devoted to study some aspects of anomalous thermodynamical state [1] called a fermion condensate. In particular, we are interested in analysing relativistic quark ensemble with a specific form of four-fermion interaction. These field theory models (QCD like models) are still most reliable source of qualitative (and quantitative) information on the transport characteristics of strongly correlated quark systems and the chiral phase transition between massive hadrons and massless quarks.

The thermodynamical description of the quark ensemble with four-fermion interaction (generated as it is believed by strong stochastic gluon fields) is grounded on the Hamiltonian density

$$\mathcal{H} = -\bar{q} (i\gamma\nabla + m) q - j_\mu^a \int d\mathbf{y} \langle A_\mu^a A_\nu^b \rangle j_\nu^b, \quad (1)$$

where $j_\mu^a = \bar{q} t^a \gamma_\mu q$ is the quark current, with operators of the quark fields q , \bar{q} , taken in spatial point \mathbf{x} (the variables with prime correspond to the \mathbf{y} point), m is the current quark mass, $t^a = \lambda^a/2$ is the color gauge group $SU(N_c)$ generators, $\mu, \nu = 0, 1, 2, 3$. The gluon field correlator $\langle A_\mu^a A_\nu^b \rangle$ is taken in the simplest color singlet form

with a time contact interaction (with no retarding)

$$\langle A_\mu^a A_\nu^b \rangle = G \delta^{ab} \delta_{\mu\nu} F(\mathbf{x} - \mathbf{y}), \quad (2)$$

(we do not include the time delta-function in this formula). This effective Hamiltonian should describe quasi-stationary states of quark ensemble and it results (in natural way) from the coarse-grained description of the system (see a derivation of vacuum gluon fields in form of the instanton liquid [2]). Relying on a point-like approximation of correlation function in coordinate space we come to the Nambu–Jona-Lasinio model (NJL) [3]. The opposite limit of infinite correlation length (δ -function like behavior in momentum space) is widely used in condensed matter physics and known as the Keldysh model [4]. Realizing that for the strongly interacting systems the size of characteristic vacuum box is found of $\Lambda_{\text{QCD}}^{-1}$ order [5] we could qualitatively expect that both opposite models lead to practically the same picture of spontaneous chiral symmetry breaking, color superconductivity and some important features, because a scale of coupling constant G can be properly tuned by using meson observables [6], [7].

It is believed (for KKB model it was proved in [5]) that at strong enough interaction the ground state of system transforms from trivial vacuum $|0\rangle$ (the vacuum of free Hamiltonian) to the mixed state (the quark–anti-quark pairs with opposite momentum with vacuum quantum numbers), which is presented as the Bogolyubov trial function (in that way some separate reference frame is introduced, and chiral phase becomes fixed)

$$|\sigma\rangle = \mathcal{T}|0\rangle, \quad \mathcal{T} = \prod_{p,s} \exp[\varphi_p (a_{p,s}^+ b_{-p,s}^+ + a_{p,s} b_{-p,s})].$$

Here a^+ , a , b^+ , b are the quarks creation and annihilation operators, $a|0\rangle = 0$, $b|0\rangle = 0$. The dressing transformation \mathcal{T} transmutes the quark operators to the creation and annihilation operators of quasiparticles $A = \mathcal{T} a \mathcal{T}^\dagger$, $B^+ = \mathcal{T} b^+ \mathcal{T}^\dagger$.

*Also at Institute of Theoretical and Experimental Physics, Moscow, RUSSIA

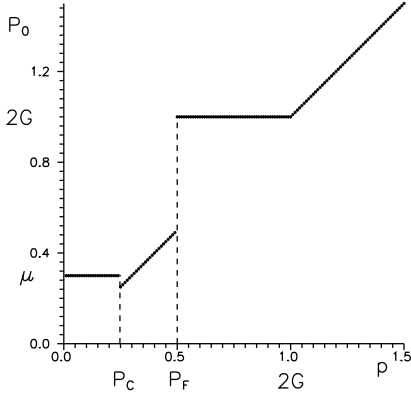


FIG. 1: Quark energy as a function of momentum for the first (see the text) solution.

The thermodynamic properties of the quark ensemble determines by solving the following problem. It should be found such a statistical operator

$$\xi = \frac{e^{-\beta \hat{H}_{\text{app}}}}{Z_0}, \quad Z_0 = \text{Tr} \{e^{-\beta \hat{H}_{\text{app}}}\}, \quad (3)$$

that at fixed mean charge

$$\overline{Q}_0 = \text{Tr}\{\xi Q_0\} = V \gamma \int d\tilde{\mathbf{p}} (n - \bar{n}), \quad (4)$$

($Q_0 = \bar{q}\gamma^0 q$), and fixed mean entropy

$$\begin{aligned} \overline{S} = & -\text{Tr}\{\xi S\} = \\ & -V \gamma \int d\tilde{\mathbf{p}} [n \ln n + (1-n) \ln(1-n) + \\ & + \bar{n} \ln \bar{n} + (1-\bar{n}) \ln(1-\bar{n})], \end{aligned} \quad (5)$$

($S = -\ln \xi$), the mean energy of the quark ensemble

$$E = \text{Tr}\{\xi H\},$$

($H = \int d\mathbf{x} \mathcal{H}$) would be minimal. In other words we are interested in finding the minimum of the following functional

$$\Omega = E - \mu \overline{Q}_0 - T \overline{S}, \quad (6)$$

where μ and T denote the Lagrangian multiplier for chemical potential and the temperature respectively ($\beta = T^{-1}$). V is a volume in which the system is enclosed, $d\tilde{\mathbf{p}} = d\mathbf{p}/(2\pi)^3$, $\gamma = 2N_c$ (in the case of quarks of a few flavors $\gamma = 2N_c N_f$, where N_f is the number of flavors), $n = \text{Tr}\{\xi A^+ A\}$, $\bar{n} = \text{Tr}\{\xi B^+ B\}$ are the components of corresponding density matrix.

We restrict ourselves by considering the Bogolyubov–Hartree–Fock approximation in which the statistical operator is constructed on the basis of approximated effective Hamiltonian H_{app} quadratic in creation and annihilation operators of quasi-particles acting in the corresponding Fock space with a vacuum state $|\sigma\rangle$. The

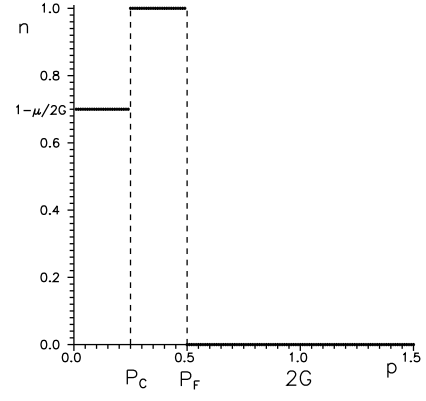


FIG. 2: Quark ensemble density as a function of the momentum for the first (see the text) solution. Fermion condensate solution is followed by the Fermi sphere, and then by the vacuum solution.

average specific energy per quark $w = E/(V\gamma)$ is given [8] by the following form

$$\begin{aligned} w = & \int d\tilde{\mathbf{p}} p_0 - \int d\tilde{\mathbf{p}} (1-n-\bar{n}) p_0 \cos \theta - \\ & - \frac{1}{2} \int d\tilde{\mathbf{p}} (1-n-\bar{n}) \sin(\theta - \theta_m) M(\mathbf{p}), \end{aligned} \quad (7)$$

where

$$M(\mathbf{p}) = 2G \int d\tilde{\mathbf{q}} (1-n'-\bar{n}') \sin(\theta' - \theta'_m) F(\mathbf{p} + \mathbf{q}),$$

$\theta = 2\varphi$, $p_0 = (\mathbf{p}^2 + m^2)^{1/2}$, the primed variables, here and below, correspond to the integration over momentum \mathbf{q} . The auxiliary angle θ_m is determined from the relation: $\sin \theta_m = m/p_0$. The first term in Eq. (7) is introduced in view of normalization in order to have the zero ground state energy when an interaction is switched off. This constant would be inessential in what follows and can be safely omitted. However, it should be kept in mind that it will appear further as a regularizer in singular expressions if they occur.

For the delta-like potential in coordinate space (NJL model) the expression (7) diverges and to obtain the reasonable results the cut-off upper limit over momentum integration Λ is introduced, which along with the coupling constant G and current quark mass m is one of the tuning model parameter. Below we use one of the standard parameter sets for the NJL model [9]: $\Lambda = 631$ MeV, $G\Lambda^2/(2\pi^2) \approx 1.3$, $m = 5$ MeV while the KKB model parameters are chosen in such a way that for the same current masses the quark dynamical masses in both NJL and KKB models coincide at vanishing quark momentum.

Using the extremal properties the functional Eq. (7)

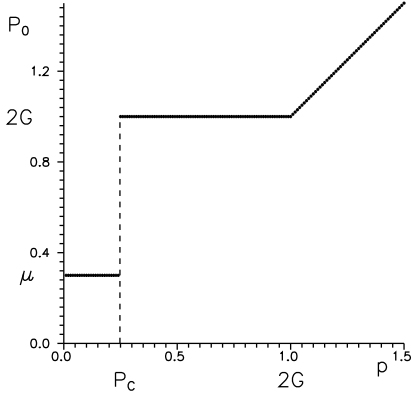


FIG. 3: Quark energy as a function of momentum for the second (see the text) solution.

can be transformed to the form (see [8])

$$w = \int d\tilde{\mathbf{p}} p_0 - \int d\tilde{\mathbf{p}} (1 - n - \bar{n}) P_0 + \frac{1}{4G} \int d\tilde{\mathbf{p}} d\tilde{\mathbf{q}} F(\mathbf{p} + \mathbf{q}) \tilde{M}(\mathbf{p}) \tilde{M}(\mathbf{q}), \quad (8)$$

where $P_0 = [\mathbf{p}^2 + M_q^2(\mathbf{p})]^{1/2}$ is the energy of quark quasiparticle with a quark dynamical mass

$$M_q(\mathbf{p}) = m + M(\mathbf{p}) = m + \int d\tilde{\mathbf{q}} F(\mathbf{p} + \mathbf{q}) \tilde{M}(\mathbf{q}). \quad (9)$$

Below we omit the arguments of corresponding functions for the mass and quasiparticle energy. Varying the functional (8) with respect to the density of induced quasiparticle mass \tilde{M} (in such a form it is convenient to calculate variational derivatives[16]) we obtain the following equation for dynamical quark mass

$$M_q(\mathbf{p}) = m + 2G \int d\tilde{\mathbf{q}} (1 - n' - \bar{n}') \frac{M'_q}{P'_0} F(\mathbf{p} + \mathbf{q}), \quad (10)$$

which exactly corresponds to the mean field approximation. In particular, under normal condition ($T = 0$, $\mu = 0$) the quark dynamical mass in NJL model is $M_q \sim 340$ MeV, while the quark dynamical mass of the KKB model is determined by the equation

$$M(\mathbf{p}) = 2G \frac{M_q(\mathbf{p})}{P_0}. \quad (11)$$

In practice it is convenient to deal with the inverse function $p(M_q)$. In particular, in the chiral limit $M_q = (4G^2 - \mathbf{p}^2)^{1/2}$ for $|\mathbf{p}| < 2G$, and $M_q = 0$ at $|\mathbf{p}| > 2G$. Then, the quark states with momenta $|\mathbf{p}| < 2G$ are degenerate in energy $P_0 = 2G$.

It was suggested in [1] that, besides the standard Fermi distribution, the anomalous states (fermion condensate) are possible. We study them here with the KKB model example discussing, first, the situation of zero temperature. We need to find a minimum of the functional (6) at

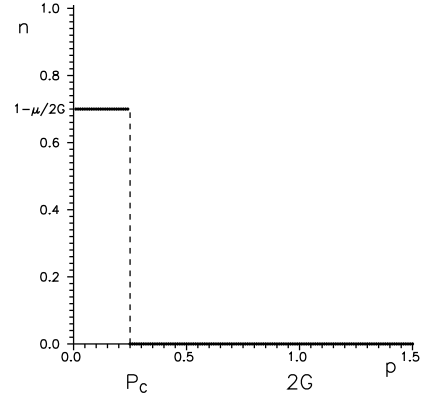


FIG. 4: Quark ensemble density as a function of the momentum for the second (see the text) solution. P_C value separates a fermion condensate and vacuum contributions.

a fixed mean charge (baryon number) $\bar{\mathcal{N}} = \gamma \int d\tilde{\mathbf{p}} n(\mathbf{p})$, and mean entropy $\bar{\mathcal{S}} = \gamma \int d\tilde{\mathbf{p}} s(\mathbf{p})$. By varying the quark dynamical mass M_q and density n we obtain the system of equations

$$\begin{aligned} -(1 - n) \frac{M_q}{P_0} + \frac{M}{2G} &= 0, \\ P_0 - \mu - T \ln(n^{-1} - 1) &= 0. \end{aligned} \quad (12)$$

For the fermi-condensate it is proposed to make use the second equation of the system (12) and search for a solution in the form

$$\begin{aligned} T &\equiv 0, \\ P_0 &= \mu, \end{aligned} \quad (13)$$

degenerate in energy (as was shown above a similar behavior is demonstrated by the KKB model). Then for the quark dynamical mass we have

$$M_q = \pm(\mu^2 - \mathbf{p}^2)^{1/2}, \quad (14)$$

and $|\mathbf{p}| < \mu$ if one is interested in the real solutions only. Besides, there exist, of course, a standard solution which is considered to be an asymptotic form of the Fermi distribution at $T \rightarrow 0$

$$n = \frac{1}{e^{\beta(P_0 - \mu)} + 1},$$

with $P_0 = [\mathbf{p}^2 + M_q^2(\mathbf{p})]^{1/2}$. The quark dynamical mass is defined by the following relations

$$\begin{aligned} \frac{M_q}{P_0} &= \frac{M}{2G}, \quad n = 0, \quad |\mathbf{p}| > P_F, \\ M &= 0, \quad n = 1, \quad |\mathbf{p}| < P_F. \end{aligned} \quad (15)$$

By definition, the condensate density satisfies inequalities $0 < n < 1$. From the first equation of the system (12) we find two possible density distributions

$$n_{\pm} = 1 - \frac{\mu}{2G} \pm \frac{\mu}{2G} \frac{m}{(\mu^2 - \mathbf{p}^2)^{1/2}}. \quad (16)$$

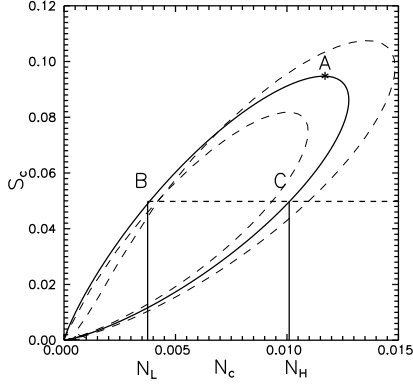


FIG. 5: The entropy density (per fm^3) as a function of quark ensemble density (per fm^3) for a fermi condensate state. The solid curve is obtained in the chiral limit, which serves as an example for examining an issue of quark ensemble density increase at fixed mean entropy.

It is interesting to note the peak in the density n_+ at $|\mathbf{p}| \sim \mu$, but at the same time the quark density cannot exceed 1. For the second solution n_- another constraint $n > 0$ is valid. Going to find the domain of the solution n_+ applicability we define the momentum p_+ in a way that $n_+ = 1$, i.e. $p_+ = (\mu^2 - m^2)^{1/2}$. It is obvious that the momentum p_+ is separated from the value μ , where the density n_+ is singular, by a constant value that is defined by the quark current mass. Defining the region of the second solution n_- applicability we define the momentum p_- to have $n_- = 0$, i.e. $p_- = [\mu^2 - m^2 \mu^2 / (2G - \mu)^2]^{1/2}$. In contrast to the momentum p_+ the limiting momentum found is movable with respect to the value μ , at $\mu \rightarrow 0$ we have $p_- \rightarrow \mu$. When $\mu = G$, the momenta p_+ and p_- coincide ($p_+ = p_-$). If $\mu = \mu_- = 2G - m$ then p_- goes to zero. For larger $\mu > \mu_-$ the second branch of solution, n_- , disappears. Summarizing, we may conclude that it is possible to have the situations in which there exist two solutions for the condensate within the interval of momenta. Then beyond this region an interval can be situated where only one solution exists either, n_+ or n_- depending on the relation between momenta p_+ and p_- . And, finally, beyond this latter interval only the solution with a standard Fermi distribution can exist.

Further analysis can be carried out in the chiral limit only. In this case both branches n_+ and n_- get merged and the condensate density does already not depend on the quark momentum

$$n = n_+ = n_- = 1 - \frac{\mu}{2G}.$$

It is seen that the condensate solution is possible only at $\mu < 2G$. Then $M_q = M = (\mu^2 - \mathbf{p}^2)^{1/2}$, and here the real solution exists only within the interval $0 \leq |\mathbf{p}| \leq \mu$. In addition to the condensate solution the standard one is also possible

$$\begin{aligned} M_q = M &= [(2G)^2 - \mathbf{p}^2]^{1/2}, & n = 0, & |\mathbf{p}| > P_F \\ M = 0, & & n = 1, & |\mathbf{p}| \leq P_F. \end{aligned}$$

It is easy to understand that the general solution can be obtained by combining the standard solutions of the Fermi step and fermion condensate at different intervals of momentum axis. We consider a few such possibilities. Figs. 1, 2 demonstrate the quark energy and quark ensemble density as the functions of momentum. We place the solution with a Fermi condensate into the interval $[0, P_C]$ localizing the Fermi sphere in the interval $[P_C, P_F]$ and vacuum solution is placed behind the Fermi momentum P_F . According to definition we take here $P_C < P_F$, $\mu \geq P_C$ and call such functions as the first solution. Detaching the solution without Fermi sphere we call it as the second solution. Figs. 3 and 4 show the corresponding quark energy and quark ensemble density. Thus, there is a fermion condensate that is followed with the vacuum solution along the momentum axis and then $\mu \geq P_C$. It could be convenient to characterize the solutions with the dimensionless variables $x = \mu/(2G)$, $y = P_F/(2G)$, $z = P_C/(2G)$. The mean entropy density and the particle number density in the fermion condensate for the second solution are given by:

$$\begin{aligned} \mathcal{S}_2 &= -\frac{\gamma}{6\pi^2} z^3 [(1-x) \ln(1-x) + x \ln x] (2G)^3, \\ \mathcal{N}_2 &= \frac{\gamma}{6\pi^2} z^3 (1-x) (2G)^3. \end{aligned} \quad (17)$$

When $\mu = P_C$ the fermion condensate contains maximally possible number of states. Fig. 5 explores the entropy density (over fm^3) of the Fermion condensate as function of baryon density $\mathcal{N} = Q_0/(3V)$, and we specify it as $2G = 300 \text{ MeV}$. The solid oval line is obtained in the chiral limit. We present it in physical units in order to estimate the order of magnitude of the characteristics. But in what follows we characterize the entropy, quark ensemble density and ensemble energy in dimensionless variables (with the corresponding powers of coefficient $2G$). Fig. 5 shows also the entropy density for the quark ensemble with current quark mass $m = 5 \text{ MeV}$. S_+ (large dashed oval), and S_- (small dashed oval) was obtained by making use the distributions n_+ and n_- correspondingly. The maximal condensate density is achieved at $x_N = 3/4$, $N_c \approx 3.56 \cdot 10^{-3} (2G)^3$, maximal entropy occurs at $x_S \approx 0.84$, $S_c \approx 2.64 \cdot 10^{-2} (2G)^3$ ($N_f = 1$). The fermion condensate states with $P_C < \mu$ populate an oval interior. The energy density of the second solution is calculated from Eq. (8) (where the integration is extended up to the boundary momentum $2G$ only because the large values of chemical potential and momentum P_C, P_F are unrealistic) in the following form

$$\mathcal{E}_2 = -\frac{\gamma}{4\pi^2} \left(\frac{8}{15} - \frac{z^3}{3} + \frac{z^3 x^2}{3} \right) (2G)^4. \quad (18)$$

The solutions obtained could be interpreted as nontrivial continuation of a standard procedure of filling in the Fermi sphere (in that case chemical potential is equal to or exceeds the dynamical quark mass by definition) up to the situation when the chemical potential values become smaller than M_q . Figs. 6 and 7 show the third

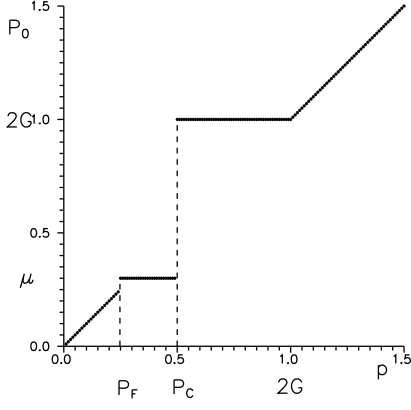


FIG. 6: Quark energy as a function of momentum for the third (see the text) solution.

solution with $P_C > P_F$, $\mu \geq P_C$. It looks like the first solution, but with momenta separating the Fermi sphere from the fermion condensate rearranged. Here we do not discuss the solution with Fermi sphere only (without fermion condensate) because the entropy of this state is equal to zero.

Then average particle number density, average entropy density and average energy density for the first solution are the following:

$$\begin{aligned}\mathcal{N}_1 &= \frac{\gamma}{6\pi^2} (y^3 - z^3 x) (2G)^3, \\ \mathcal{S}_1 &= -\frac{\gamma}{6\pi^2} z^3 [(1-x)\ln(1-x) + x\ln x] (2G)^3, \\ \mathcal{E}_1 &= -\frac{\gamma}{4\pi^2} \left(\frac{8}{15} - \frac{y^3}{3} + \frac{z^3 x^2}{3} + \frac{z^5}{5} - \frac{y^5}{5} \right) (2G)^4.\end{aligned}\quad (19)$$

Similar quantities for the third solution look like:

$$\begin{aligned}\mathcal{N}_3 &= \frac{\gamma}{6\pi^2} (z^3(1-x) + y^3 x) (2G)^3, \\ \mathcal{S}_3 &= -\frac{\gamma}{6\pi^2} (z^3 - y^3) [(1-x)\ln(1-x) + x\ln x] (2G)^3, \\ \mathcal{E}_3 &= -\frac{\gamma}{4\pi^2} \left(\frac{8}{15} - \frac{z^3}{3} + \frac{(z^3 - y^3)x^2}{3} - \frac{y^5}{5} \right) (2G)^4.\end{aligned}\quad (20)$$

In order to find the minimal energy at fixed average entropy, and the average quark ensemble density we analyze auxiliary function $[-(1-x)\ln(1-x) - x\ln x]$. This function develops the maximal value $\ln 2$ at the point $x = 0.5$ and at the point $x = 0$ and $x = 1$ it possesses the minimum value equal to zero. There are two roots of equation $[-(1-x)\ln(1-x) - x\ln x] = c$ for $0 < c < \ln 2$ and due to symmetry arguments, the second root for $x > 0.5$, $x_2 = 1 - x_1$ is obviously determined by the root x_1 for $x < 0.5$. As the "reference" solution we consider the second one, because it is simpler to realize a searching algorithm considering the relations (18) as a system of equations for x and z . (Then the similar analysis could be fruitfully to the first and third solutions.) At a fixed entropy $0 < \mathcal{S} < \mathcal{S}_{\max}$ the condensate solution is located in the interval B , C , see Fig. 5. Making use a

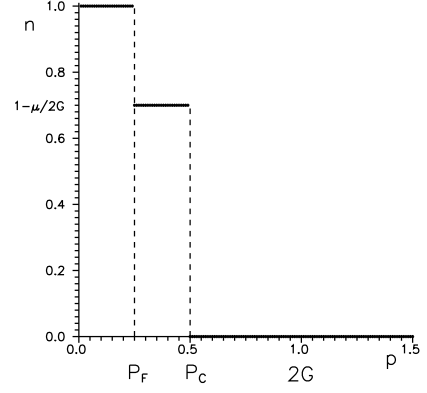


FIG. 7: Quark ensemble density as a function of the momentum for the third (see the text) solution. The fermion condensate and Fermi sphere are rearranged here comparing to the first solution, see Fig. 2.

standard method of interval bisection we are searching particular value of auxiliary function— c . This value c is fixed by a constraint to have z^3 (defined by the corresponding x and running value \mathcal{N}_C) from the first line of Eq. (18) in coincident (within required precision) with z^3 from the second line. (It is clear that both branches of the auxiliary function mentioned above should be taken into account.) Obviously, the similar construction (Eq. (18)) could be applied for the first solution analysis, but should be added by the contributions of the states falling into the Fermi sphere

$$\mathcal{N}_1 = \frac{\gamma}{6\pi^2} [y^3 - z^3 + z^3(1-x)] (2G)^3.$$

Actually, it is more convenient to realize that in two steps. First, we define x and z at $\mathcal{N}_L \leq \mathcal{N}_C \leq \mathcal{N}_R$, then at the second step $0 \leq \mathcal{N}_F \leq \mathcal{N}_B - \mathcal{N}_C$ where \mathcal{N}_B denotes a maximal quark ensemble density and

$$\mathcal{N}_F = \frac{\gamma}{6\pi^2} (y^3 - z^3),$$

we determine y . The total density of the quark ensemble is:

$$\mathcal{N} = \mathcal{N}_C + \mathcal{N}_F.$$

Similarly, one can deal with the third solution. It is seen from Eq. (20) that now in the "reference" algorithm instead of z^3 the of $z^3 - y^3$ appears

$$\mathcal{N}_3 = \frac{\gamma}{6\pi^2} [y^3(z^3 - y^3)(1-x)] (2G)^3,$$

where the state density of the Fermi condensate is

$$\mathcal{N}_F = \frac{\gamma}{6\pi^2} y^3.$$

Then the total ensemble density is defined as $\mathcal{N} = \mathcal{N}_C + \mathcal{N}_F$. We passed all the steps for the first solution similarly to the analysis done above.

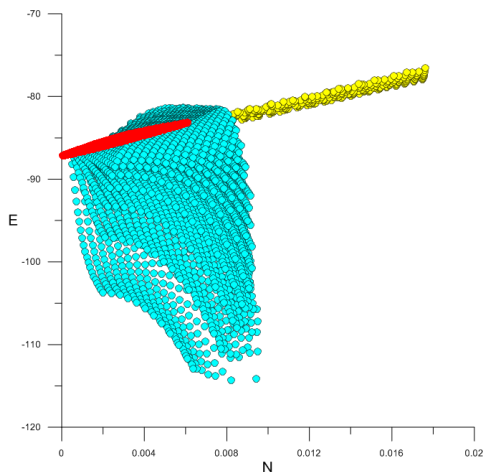


FIG. 8: Energy density as a function of the quark density of the ensemble for the three solutions.

Further, proceeding to the qualitative analysis we are based on the knowledge of the state energies as a function of quark/baryon ensemble density (in fm^3) (baryon density is in factor three smaller than the quark one) putting those on the \mathcal{E} — \mathcal{N} plane, Fig. 8. (The thorough analysis supposes a consideration of envelope of the curves.) The red region in this Fig. 8 corresponds to the second solution, and shows the quark ensemble state at low densities, where (at non-zero entropy) the contribution of the Fermi sphere is significantly suppressed. At the densities $\mathcal{N} \sim 4 \cdot 10^{-4} - 5 \cdot 10^{-4}$ (in dimensionless units) the contribution of the states filling in the Fermi sphere, which are described by third solution (blue dots in Fig. 8), starts to increase.

Characteristic values of the other parameters are the following: $x \sim 0.25$, $z \sim 0.18$ (for the second solution) and $x \sim 1$, $y \sim 0.15$, $z \sim 0.4$ (for the third solution). The density of fermion condensate is estimated to be high $n \sim 0.7$ in the second solution and for the third solution it is lower, however the process of filling in the Fermi sphere provides quite noticeable impact. It looks like that at such densities the quarks spill over from the fermion condensate into the Fermi sphere. At further increase of ensemble density the process of the Fermi sphere filling in with the fermion condensate is described by the first solution (yellow dots in Fig. 8). Characteristic ensemble densities when the transition from the state in which the fermion condensate is available at large momenta (see Fig. 7) to the state where the fermion condensate exist at small momenta (see Fig. 2) are estimated as $\mathcal{N} \sim 8 \cdot 10^{-3}$ with $x \sim 1$, $y \sim 0.15$, $z \sim 0.4$ (for the third solution) and $x \sim 0.2$, $y \sim 0.4$, $z \sim 0.2$ (for the first solution).

It means that in the region of large momenta the low density fragment of fermion condensate (resulting from the third solution) spills over into low momenta region (resulting from the first solution) reaches remarkable density $n \sim 0.8$. This rearrangement of quark ensemble behavior is accompanied by relatively high energy release

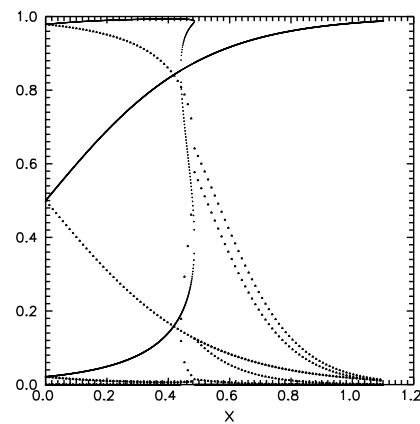


FIG. 9: Five branches of solutions to Eqs. (24), (25) for the quark and anti-quark densities (which correspond to the curves with lower density of dots) with parameter $y = 0.25$ as a function of the parameter x .

(absorption) of order about $20 \text{ MeV}/\text{fm}^3$ (with $2G = 300 \text{ MeV}$). Analysis of a general solution including an alternation of different fragments of the fermion condensate and the Fermi sphere is quite complicated, and it is a reason why we are focused only on the analysis done above. It was also mentioned that spontaneous breaking of chiral symmetry and other possible phase transitions take place in a similar way in both NJL and KKB models. It is easy to show that a similar situation happens to a fermion condensation considered here, albeit we argued it dealing with the KKB model only. The visible difference is that instead of a constant quark energy characteristic for the KKB model (easily seen in Figs.) the parabolic structures appear which correspond to the constant quark mass (just an approximation in which the NJL model is valid). However we are not calculating it here and refer to the result of Ref. [6].

Now turning to the situation of final temperature we restrict ourselves to analyzing the solutions in the chiral limit only and keeping in mind that the limit $T \rightarrow 0$, as we see, leads to an essentially singular point. Then an explicit dependence on the momentum is absent that makes of course a considerable convenience for analysis. Here it is necessary to take into account the anti-quark contribution resulting in the system (12) to get the form

$$\begin{aligned} -(1 - n - \bar{n}) \frac{M_q}{P_0} + \frac{M}{2G} &= 0, \\ P_0 - \mu - T \ln(n^{-1} - 1) &= 0, \\ P_0 + \mu - T \ln(\bar{n}^{-1} - 1) &= 0. \end{aligned} \quad (21)$$

In the chiral limit we have

$$1 - n - \bar{n} = \frac{P_0}{2G}. \quad (22)$$

It is curious to note already at this point that now it becomes possible to have the situations with negative quark energy, i.e. formally it corresponds to the bound

state of a quasi-particle. The energy of quasi-particle with non-zero dynamical mass is constrained by the inequalities $-2G < P_0 < 2G$. For quarks with higher energies, $P_0 > 2G$, the first equation of the system leads to the trivial solution with zero quark dynamical mass $M_q = M = 0$. From the second equation (21) we have

$$P_0 = \mu + T \ln(n^{-1} - 1) . \quad (23)$$

For convenience, we introduce another dimensionless variables $x = \mu/(2G)$, $y = T/(2G)$ and substituting the energy in Eq. (22) we obtain

$$1 - n - \bar{n} = x + y \ln(n^{-1} - 1) . \quad (24)$$

Linking up the third equation of the system (21) we can explicitly find the density of anti-quarks as

$$\bar{n} = \left(e^{2x/y + \ln(n^{-1} - 1)} + 1 \right)^{-1} , \quad (25)$$

and putting it in Eq. (24) allows us to derive a final transcendental equation to be used in computations. To give an illustration we make use the dimensionless variables, i.e. all the characteristics to be divided by the corresponding powers of parameter $2G$. Fig. 9 displays five solutions to Eqs. (24), (25) for the quark and anti-quark densities (the dots on the curves are sparser) with parameter $y = 0.25$ as a function of parameter x . The number of branches of the transcendental equations system evolves with a change of parameter y . The chosen value $y = 0.25$ corresponds to the most abundant number of roots (remember that at zero temperature and beyond the chiral limit there were only two branches of solutions for the density). It is also interesting to mention that there appear the states with higher anti-quark density at rather moderate temperatures. Fig. 10 illustrates the mentioned possibility of having the solutions with negative quark energy which are exactly due to the considerable anti-quark contribution. (An observed value of the charge density is given by the difference of two large numbers n and \bar{n} .) A nontrivial solutions for the condensate should satisfy the energy constraint $|P_0| < 2G$. The figure also shows the straight line $P_0 = 2G$. Its intersection point with the curve gives a limiting value of the chemical potential, at which the quark condensation (generation of the quark dynamical mass) for the considered branch of solution is still possible. In the figure this point is denoted as x_r . Now we define some integral characteristics of the quark ensemble. For example, the mean charge and entropy densities look like

$$\begin{aligned} \mathcal{Q}_0 &= \gamma \int d\tilde{\mathbf{p}} (n - \bar{n}) , \\ \mathcal{S} &= \gamma \int d\tilde{\mathbf{p}} (s + \bar{s}) . \end{aligned}$$

By definition, the energy is expressed by the quark dynamical mass as

$$P_0 = \begin{cases} \pm (\mathbf{p}^2 + M^2)^{1/2} , & |P_0| \leq 2G , \\ \pm |\mathbf{p}| , & |P_0| > 2G . \end{cases}$$

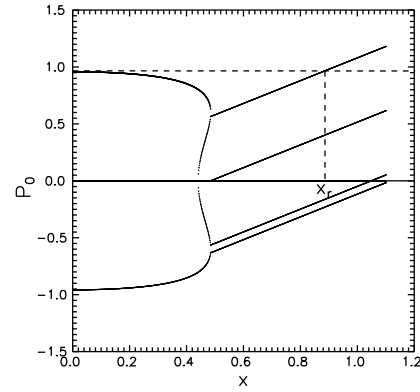


FIG. 10: The quark energy P_0 for solutions presented in Fig. 9. One may see the roots with negative energy.

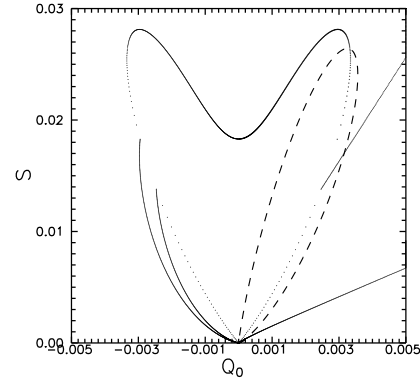


FIG. 11: The entropy density as function of the density of baryon charge, at temperature $y = 0.25$. Dashed line corresponds to the situation of zero temperature, see Fig. 5.

Here the quark momentum $|\mathbf{p}|$ is running within the interval from 0 up to $|P_0|$. Then we have

$$\begin{aligned} \mathcal{Q}_0 &= \frac{\gamma}{6\pi^2} |P_0|^3 (n - \bar{n}) , \\ \mathcal{S} &= \frac{\gamma}{6\pi^2} |P_0|^3 (s + \bar{s}) , \end{aligned}$$

with $P_0 = 2G [x + y \ln(n^{-1} - 1)]$.

Fig. 11 shows the entropy as a function of charge density at temperature $y = 0.25$ when the largest number of solutions to Eq. (21) is revealed in the chiral limit. In order to compare the dashed line demonstrates an oval obtained at zero temperature which was discussed above. Its evolution with temperature increasing can clearly be traced. The changes take place mostly due to the contribution of anti-quarks and are seen to affect the left hand branch of an oval. The right hand part of oval stays sort of more conservative. In this sense it is possible to say that with an increasing temperature of ensemble there exist some temperature window where substantial asymmetry in quark/anti-quark ensemble is manifested. With these amazing results, we limit our analysis in the present paper. In order to examine the state of ensemble as a function of mean entropy and mean charge in a way

similar to what was done in the situation of zero temperature, it is necessary to analyse more carefully the chiral limit, $m \rightarrow 0$, of solutions to the equation system (21). We demonstrate the states of ensemble with the fermi-condensate at the temperature approaching the absolute zero may occupy the whole semi-plane bounded at the $S - N$ plane by maximal value of accessible entropy $S < S_c$. (In fact, this result could be considered as another example of the Nernst 'heat theorem' breakdown that has been predicted for strongly correlated fermi-systems of condensed matter physics [1], [11].

Here, it is worth to remind one remarkable fact for those who is interested in further development of such an approach. The models of similar Hamiltonian forms were (and are) widely used in the physics of condensed matter and nuclear physics while dealing with the ensembles of finite particle numbers. They are exactly integrable [12], [13] and well understood in the framework of conformal theory [14]. It encourages us to construct a field theory model with an increasing correlation length to trace back, in a sense, field theory origin of the BCS-type phenomena and, perhaps, to develop a fresh look at the deconfinement conception.

Summarizing we would like to emphasize that our unexpected point in this paper concerns the statement about the possible rearrangement of the quark ensemble with energy release (absorbption) about 20 MeV/fm³ (for $2G = 300$ MeV) at its density increasing. It seems this rearrangement of quark ensemble could be instrumental

in the astrophysical applications, in particular, to study the problem of Supernova outburst [15].

These solutions to the system of thermodynamic equations are quite different from the standard ones because of very high ensemble density that in considerable extent is caused by significant contribution of anti-quarks. Our ensemble displays the features which are shared by, for example, the unitary Fermi gas and could be pretty universal. The latter is considered as one of the strongest correlated systems in the nature because it saturates the unitary bound for the $s - wave$ cross section and develops, as known, the features similar to QGP. We hope to return to discussing these problems in more general context of quantum phase transitions and anomalous behavior of Fermi-systems [11] in future, and now concluding we would like to mention that going to perform a similar analysis of Fermi condensate in the NJL-model we have to deal with the non-local formulations. The remarkable advantage of our analysis here (which can be quite practical in studying an origin of turbulence in QGP) is the locality of interaction in the momentum space.

ACKNOWLEDGMENTS

Authors are deeply indebted to K. A. Bugaev, I. M. Dremin, V. V. Goloviznin, E.-M. Ilgenfritz, A. V. Leonidov, D. K. Nadezhin, S. N. Nedelko, V. V. Skalozub, A. M. Snigirev and many other colleagues for numerous fruitful discussions. The work was partially supported by the State Fund for Fundamental Research of Ukraine, Grant № Ph58/04.

-
- [1] V. A. Khodel and V. R. Shaginyan, JETP Letters **51** (1990) 553;
V. A. Khodel and V. R. Shaginyan, Phys. Rep. **249** (1994) 1.
 - [2] S. V. Molodtsov and G. M. Zinovjev, Phys. Rev. **D80** (2009) 076001;
 - [3] Y. Nambu and G. Jona-Lasinio, Phys. Rev. **122** (1961) 345.
 - [4] M. V. Sadovskii, Diagrammatics, Singapore: World Scientific, 2006.
L. V. Keldysh, Dr. Hab. thesis (FIAN, 1965);
E. V. Kane, Phys. Rev. **131** (1963) 79;
V. L. Bonch-Bruевич, in 'Physics of solid states', M., VINITI, 1965.
 - [5] S. V. Molodtsov, G. M. Zinovjev, arXiv:1406.5561 [hep-ph].
 - [6] G. M. Zinovjev, S. V. Molodtsov, Physics of Atomic Nuclei, **77** (2014) 743.
 - [7] G. M. Zinovjev and S.V. Molodtsov, Phys. Atom. Nucl. **75** (2012) 239;
G. M. Zinovjev, M. K. Volkov and S.M. Molodtsov, Theor. Math. Phys. **161** (2009) 1668; arXiv:0812.2666.
 - [8] S. V. Molodtsov and G. M. Zinovjev, Europhys. Lett. **93** (2011) 11001; Phys. Rev. **D84** (2011) 036011;
 - [9] T. Hatsuda and T. Kunihiro, Phys. Rep. **247** (1994) 221.
 - [10] H. Tezuka, Phys. Rev. **C22** (1980) 2585; **C24** (1981) 288;
G. Baym and S. A. Chin, Nucl. Phys. **A262** (1976) 537;
T. Matsui, Nucl. Phys. **A370** (1981) 369.
 - [11] V. R. Shaginyan, M. Ya. Amusia and K. G. Popov, Phys.-Usp. **50** (2007) 563;
C. M. Stishov, Phys.-Usp. **47** (2004) 789.
 - [12] R. W. Richardson, Phys. Lett. **3** (1963) 277;
R. W. Richardson and N. Sherman, Nucl. Phys. **B52** (1964) 221;
R. W. Richardson, J. Math. Phys. **6** (1965) 1034.
 - [13] M. Gaudin, J. Physique **37** (1976) 1087;
M. C. Cambiaggio, A. M. F. Rivas and M. Saraceno, Nucl. Phys. **A624** (1997) 157.
 - [14] G. Sierra, Nucl. Phys. **B572** (2000) 517;
J. Dukelsy, S. Pittel and G. Sierra, Rev. Mod. Phys. **76** (2004) 643.
 - [15] M. I. Krivoruchenko, D. K. Nadyozhin, T. L. Rasinkova, Yu. A. Simonov, M. A. Trusov, and A. V. Yudin, Phys.Atom.Nucl. **74** (2011) 371.
 - [16] If one takes the quark dynamical mass M_q as a basic variable, then it is seen from Eq. (9) that it is difficult to formulate an inverse transformation from M_q to \widetilde{M} suitable for handling.